Springer

KSME

Journal of Mechanical Science and Technology 24 (7) (2010) 1501~1509
www.springerlink.com/content/1738-494x
DOI 10.1007/s12206-010-0501-6

Experimental study on nanofludic heat pipe hot chuck plate in semiconductor wafer baking process [†]

Taek-Kyu Lim and Seok-Ho Rhi[*]

School of Mechanical Engineering, Chungbuk National University, Cheongju, Chungbuk, 361-763, Korea

(Manuscript Received July 7, 2009; Revised Marh 11, 2010; Accepted May 2, 2010)

Abstract

The temperature uniformity on a heat pipe hot chuck (HPHC) during semiconductor wafer processing has been an important factor to critical dimension (300 mm) uniformity as the feature size of semiconductors decreases and productivity density increases due to the new process of nano size special manufacturing technology. To design the present heat pipe hot chuck system, which has enhanced temperature uniformity for the wafer process, the heat distribution of the system was analyzed experimentally with various working fluids such as water, TiO_2, ATO, ITO, Al_2O_3, and Ag-nanofluids and 8 cell structures. Unlike the conventional solid state chuck, the present heat pipe hot chuck system consists of a heat pipe containing specially charged working fluid. Various working fluids have been tested to find best temperature uniformity feature on the top surface of hot chuck. TiO_2-nanofluid was used and tested as the working fluid of the heat pipe hot chuck system in this paper. The temperature uniformity of upper surface was sustained in the range of $\pm 1^oC$. A nano-porous layer was observed on the surface with the good result of surface temperature uniformity compared with distilled water.

Keywords: Flat heat pipe; Hot chuck; Wafer; Nanofluid; Nano porous

1. Introduction

In recent years, the semiconductor manufacturing industry has moved to the nanotechnology or much higher technology. Furthermore, due to the high end lithography pattern technology, chip devices continue to evolve toward much smaller features. As the chip size shrinks with thin patterning process, precise temperature control technology has been getting more important and this has led to a growing demand in microfabrication processes. The recent chip density leads to wide wafer plate processing to 300 mm and 450 mm. Wide working space of wafer baking can make it difficult to control temperature uniformity. The precise temperature control for a hot chuck system wider than 300 mm is not yet studied in strength [1-3].

In the wafer tracks, both steady-state temperature uniformity and transient wafer baking temperature non-uniformity significantly impact the critical dimension uniformity. Further reduction in across-wafer and wafer-to-wafer critical dimension variation requires wafer-to-wafer baking temperature uniformity for the entire baking cycle [4-6].

The present study is on the hot chuck plate system using a nanofluidic heat pipe for baking system with 300 mm (12 inch) wafer baking tracks. The HPHC (heat pipe hot chuck) performs exceptionally well with a surface temperature distribution accuracy of $\pm 1^oC$ and superior thermal response so the entire surface of the plate heats uniformly as temperature is increased. This minimizes thermal distortion, improves temperature uniformity across the surface of the wafer, and provides uniform thermal effects on the wafer throughout the baking process, not only at steady state but also at transient state. [1-3, 6-12]

The present HPHC is operated by liquid-vapor phase changing of a two-phase closed thermosyphon (TCT). This closed two-phase changing process utilizes the latent heat of vaporization to transfer heat from the hot section with very small temperature gradients. Heat at the lower portion of a HPHC vaporizes the working fluid. During this phase change process, the fluid picks up the heat associated with its latent heat of vaporization. The vapor in the evaporator region is at a higher temperature. Hence at a higher pressure than the vapor pressure in the condenser, the vapor rises with aid of buoyancy forces and flows to the condenser where it gives up the latent heat of vaporization. The gravitation then causes the condensate film to flow back down the inside wall of the HPHC and the process repeats. This two-phase working state is the main advantage to be adapted to the present HPHC system. Although the inside surface of the HPHC may occasion-

[†] This paper was recommended for publication in revised form by Associate Editor Dongsik Kim
[*]Corresponding author. Tel.: +82 43 261 2444, Fax: +82 43 263 2441
E-mail address: rhi@chungbuk.ac.kr
© KSME & Springer 2010

ally be lined with a cell structure to promote the return of the condensate to the evaporator or to increase the associated heat transfer coefficient, an HPHC basically depends on the local gravitational acceleration for the return of the liquid from the evaporator to the condenser. Therefore, for proper operation, the evaporator of an HPHC must be located below the condenser, because dryout of the evaporator may occur. And the heat transfer characteristics of a HPHC are limited by a host of thermophysical constraints, including the thermal properties of the working fluid [13, 14].

Researches on the hot chuck plate system have been studied in Korea eagerly, because the semiconductor industries are advanced and very active. The hot chuck system has been studied rarely. Gyu Jin Park et al. [7] developed a hot plate device for hot embossing nano-imprinting machines. The conventional hot plate requires rapid heating-up, high temperature uniformity and precise controllability of temperature. An additional concern particularly for hot embossing is rapid cooling-down of the hot plate, which is essential in the demolding process. Analysis of design requirements leads to a 120mm×120mm×16mm rectangular plate made of Aluminium alloy, which has a series of cartridge heaters and circular holes for gas cooling in parallel. Park et al. [8] and Lee et al. [9] reported the possibility and reality of the thermal control on the hot plate using a CFD code. Numerical computation has been conducted for assessing the feasibility of a hot plate (l20×120 mm^2, circular plate of ϕ = 200 mm for S. Y. Lee). Parallel experiments have also been performed for verifying thermal performance. This not only shows the results the optimum number of thermocouples related to controllers but also suggests that the thermal simulation using a CFD code would be an alternative method to design and develop the thermal control equipment. J. Lee et al. [10] investigated the temperature uniformity on a wafer during post-exposure baking (PEB) process in photolithography. It has been an important factor to critical dimension (CD) uniformity as the feature size of semiconductors decreases. The need for the multi-zone hot plate and the possibility of the temperature non-uniformity on the multi-zone hot plate was explained. G. J. Park et al. [11] carried out the numerical investigation of thermal control of a hot plate device (240×240 mm^2) specially designed for thermal nanoimprint lithography with single circular heat pipes. In this study, a numerical experiment is conducted to simulate unsteady thermal behavior of hot plate under control. They introduce the possibility and reality of the thermal control on the hot plate using a CFD code (Fluent). Heat pipe is used to ensure high temperature uniformity.

J. H. Boo et al. [12] investigated the effect of condenser temperature on the disk type heat pipe. They carried out the test of temperature uniformity on the top surface in the heat pipe with FC-40 and PF5060 as the working fluid. They reported that the temperature uniformity is affected by the operating height of vapor space, the wall thickness of condenser, and the existence of wick structure.

A nanofluid which is used in the present HPHC system is a suspension of ultrafine particles in a conventional base fluid which enhances the heat transfer characteristics of the original fluid. [15-18]. Nanofluids have been studied in-depth since firstly debuting. But there are only a few published articles on deriving the boiling heat transfer of nanofluids [17, 18]. The purpose of this article is to pioneer and apply for a new application of the nanofluids. An innovative idea applied to the wafer heat pipe hot chuck system is to suspend ultrafine solid particles in the fluid for improving the thermal physical properties of a fluid.

Table 1. Working Fluids used in HPHC.

Working Fluids	Particle Concentration (α)	Charging Ratio (V^+)
ATO (Antimony Tin Oxide, Sb_2O3-SnO_2)	0.005, 0.01, 0.05, 0.1	0.1, 0.4
ITO (Indium Tin Oxide, In2SnO5)	0.005, 0.01, 0.05, 0.1	0.1, 0.4
Al_2O_3	0.005, 0.01, 0.05, 0.1	0.1, 0.4
Ag	0.005, 0.01, 0.05, 0.1	0.4
TiO_2	0.1	0.1, 0.2, 0.3, 0.4, 0.5
Pure Water		0.1, 0.2, 0.3, 0.4, 0.5

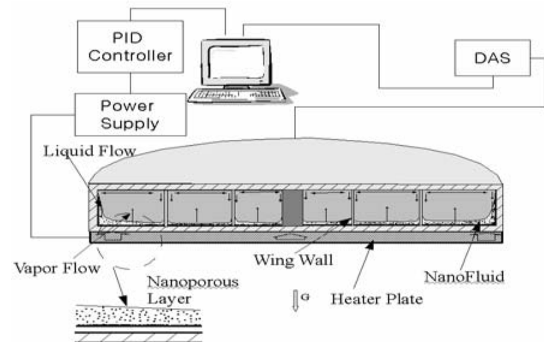

Fig. 1. Experimental setup of hot chuck test system.

It was found that only a few papers have discussed on the heat transfer of nanofluids in a real application such as heat pipes. Chien et al. [19] reported the experimental results with heat pipe using Au-water nanofluid and the average decrease of 40% in thermal resistance compared to that of pure water. Tsai et al. [20] and Kang [21] investigated heat pipes using the Au and Ag-nanofluid and reported 37% lower thermal resistance compared to that of distilled water with various heat pipes and nanofluid concentrations. They reported that smaller nanoparticles have greater reduction in thermal resistance.

Ma et al. [22] studied the nanofluid behavior in an oscillating heat pipe and thus they reported that nanofluid can reduce thermal resistance and increase critical heat flux.

In the present study, the possibilities improving the heat transfer and operation performance using HPHC with nanofluid were investigated. A hot chuck system of special design was manufactured to test various parametric effects such as kinds of working fluids, charging amount, and operation.

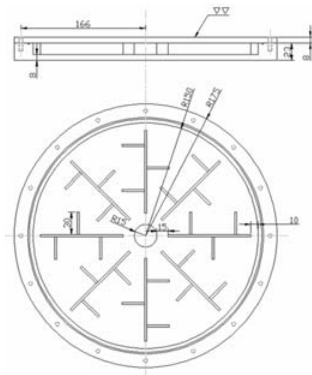

Fig. 2. Structural view of hot chuck.

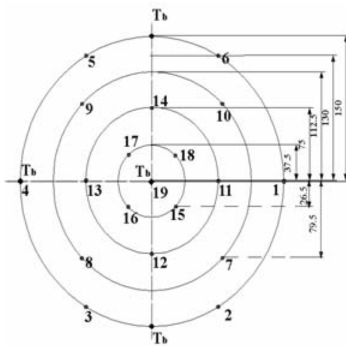

Fig. 3. Thermocouple positions on upper surface.

2. Heat pipe hot chuck element design

2.1 Experimental apparatus and method

Here we will present an overview of the structure and working principle of the heat pipe hot chuck (HPHC) plate and highlight the thermal performance of our heat-pipe plate. Fig. 1 shows schematic features of the test section and a schematic cross-section of the heat-pipe hot chuck plate. Experimental apparatus consists of HPHC, data acquisition unit, and heating unit. The HPHC plate is made of Aluminum 701 with various working fluids listed in Table 1. On the underside of the HPHC a hollow compartment is formed being integrated with an evaporator and a heater. After the HPHC is evacuated, it must be filled with a certain amount of the working fluid. An electric heater is installed in the evaporator that vaporizes the working fluid in the evaporator. This working fluid vapor condenses on the underside of the plate, which uniformly heats the surface of the plate and the wafer that is placed on the top of the HPHC plate.

The effective diameter of HPHC system is 300 mm, and inside depth is 15 mm. 25 mm margin of system is width for jointing between upper plate and bottom plate. As shown in Table 1, distilled water and TiO_2, ATO (Antimony Tin Oxide), ITO (Indium Tin Oxide), Al_2O_3 and Ag nanofluids were used for the working fluid, and its optimum amount is determined by the preliminary experimental results. 10-50% of working fluid is charged into heat pipe hot chuck, Fig. 2

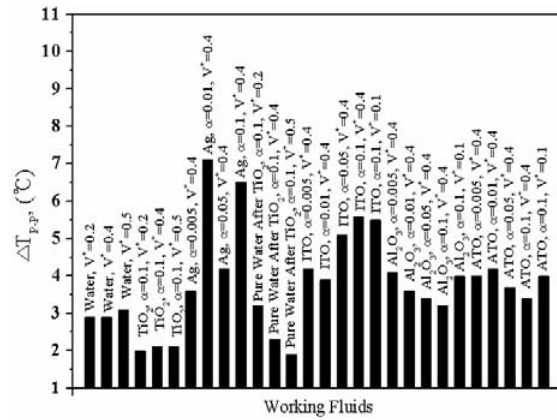

Fig. 4. Peak to peak temperature difference ($\Delta T_{p\text{-}p}$) on upper surface.

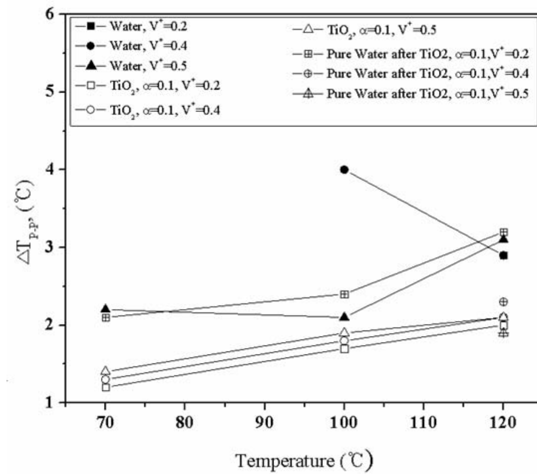

Fig. 5. Peak to peak temperature difference ($\Delta T_{p\text{-}p}$) on upper surface with different working temperature levels.

shows the specification of the heat pipe and experimental conditions. Power is supplied to nichrome wire, which is placed in the bottom of the hot chuck plate. The hot chuck and heater were assembled together. And the input power was controlled by the variable voltage adjuster and PID (proportional integral derivative) temperature controller attached to the hot chuck. The heater once insulated with the insulation plate. The temperature in the vicinity of the heating plate and the outside temperature are measured to calculate heat loss.

Power units are rated at 220V-5kW for plug-in to the heat pipe hot chuck. The robust heating element is pressed into the bottom surface of hot chuck to provide efficient heat transfer and uniform surface temperatures. The element is end sealed to resist moisture and contamination during use.

A thermostat senses the plate temperature of the chuck bottom surface to control the temperature of the top surface. The physical characteristics of the HPHC assembly used in the study are divided into three parts: the evaporation section with the evaporator bottom plate, the short smooth transporting sections, and the top surface condensing plate. The surface of the top condensing plate is main wafer baking place to sustain temperature uniformity.

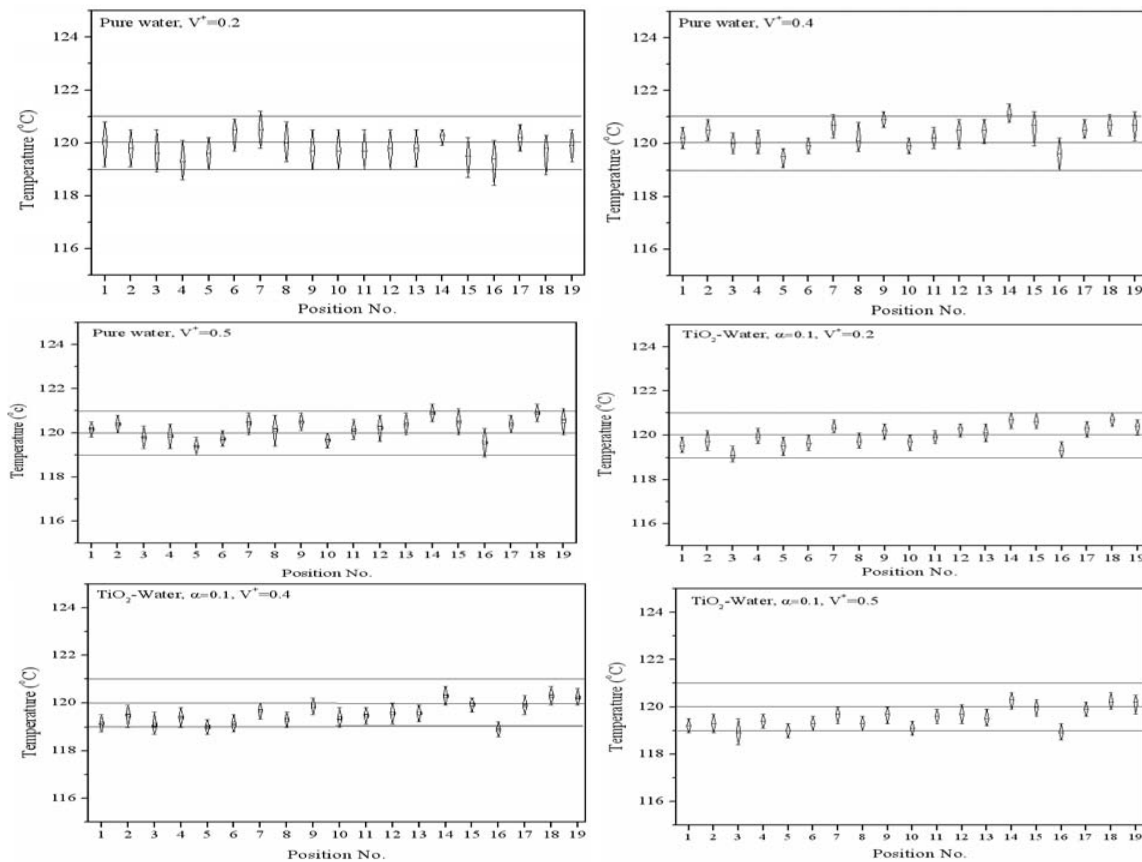

Fig. 6. Peak to Peak Temperature Difference (ΔT_{P-P}) on Upper with Different V^+, T_{Level} = 120°C.

A completely new design of the heat pipe hot chuck was developed based on a novel yet simple concept. The system was made of Aluminium 701. As shown in Fig. 2, HPHC has a particular cell structure to do modular operation inside. The upper plate of the system was 8 mm thick for both models, and the upper plate was jointed to lower container with 8 bolts and temporally sealed ϕ=5 mm circular silicon ring. A temporary seal of the test HPHC was made with a vacuum pump (PJ KODIVAC) so that the test HPHC could be used repeatedly.

To measure the temperature distribution on the surface of HPHC, 19 K-type thermocouples (ϕ=0.25mm) were used as shown in Fig. 3, and 5 K-type thermocouples were attached to the bottom of hot chuck to check and control supply power. The charging system consists of a vacuum pump, a McLeod gauge, vacuum valves and a special syringe to charge the desired amount of the working fluid into the test TCT. Pure distilled water and nanofluids as the working fluids were prepared to fill into the TCT. Nanofluids used in this work are listed in Table 1, which were supplied by NanoANP Co, Korea. De-ionized water was used as the base liquid.

The evaporator section of the hot chuck was designed to simplify the manufacturing process. Fourteen holes in the evaporator were drilled through the upper plate into the bottom side for the hot chuck plate, which connect the short adiabatic section. The center holding column (30 mm diameter) was placed in the center of the bottom side with one drilled hole to connect the upper plate. The test hot chuck assembly with the heater was installed on the desk board and covered with thick insulated wafer operation chamber.

At the start of this investigation, the transient temperature variation of the test system was recorded on computer based data acquisition system (MX100 Yokogawa). The noise was specified to be a maximum of ± 2% rms.

The power to the evaporator heating section was controlled by PID system and increased carefully in steps to the desired heat flux to satisfy operation level temperature of the top surface (70, 100, 120°C). Voltage was seen to fluctuate within a range of ± 0.2 V.

We propose an 8 radial zone design for the hot chuck plate with distinguishing walls as shown in Fig. 2, configured by properly divided zone. Each zone could act as respective heat pipe zone. Even though each zone was not a closed cell, 8 different working zones are operating as separated heat pipes.

3. Experimental results

Fig. 4 shows the temperature uniformity for the present systems with different working fluids and charging ratios. An important constraint in the operation of a HPHC is the effect of V^+ as shown in Eq. (1) In the present study, the charging ratio of the working fluid inside an HPHC is defined as the

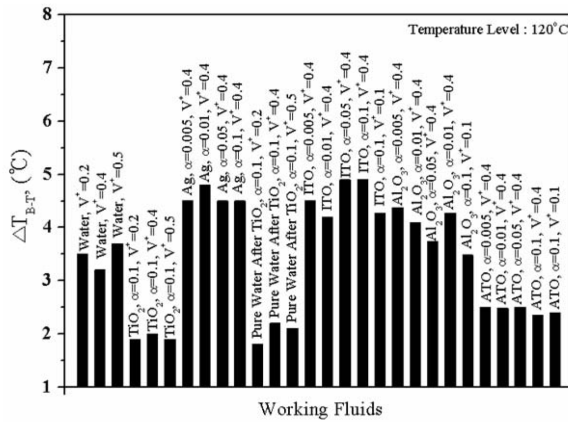

Fig. 7. Temperature difference between bottom and top surface.

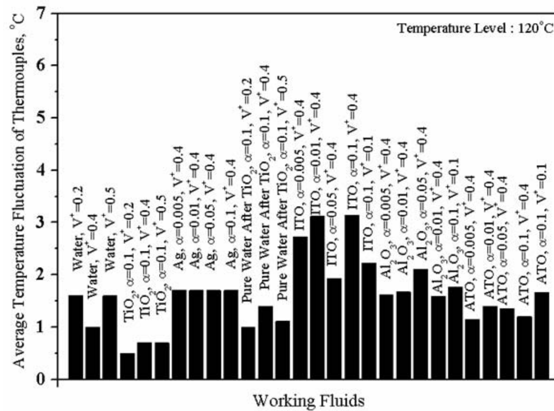

Fig. 8. Average temperature fluctuation on upper surface.

ratio of the volume of working fluid (V_{LP}) at the ambient condition to the inside volume (V_{HPHC}, effective total volume is 0.00105 m^3):

$$V^+ = \frac{V_{LP}}{V_{HPHC}} \tag{1}$$

For an HPHC, the estimation of the optimum amount of a working fluid is usually based on an assumption that the two-phase flow heat transfer in an HPHC takes place and the heat transfer in the evaporator is that of the pool boiling, whereas the evaporative heat transfer is taking place from the falling condensate liquid film above the pool of the working fluid. There are several analytical studies on the amount of working fluids in heat pipes or two-phase closed thermosyphons based on very simplified assumptions, but they all grossly underestimate the real situations [13-14]. But the present HPHC is a heat pipe and the objectives to be investigated are much different from the conventional heat pipes. The present HPHC is not only a heat transfer device, but also a temperature control system. The main purpose of HPHC is to control temperature in terms of temperature uniformity and stability on wafer baking process.

However, for HPHC, this issue is not well documented in

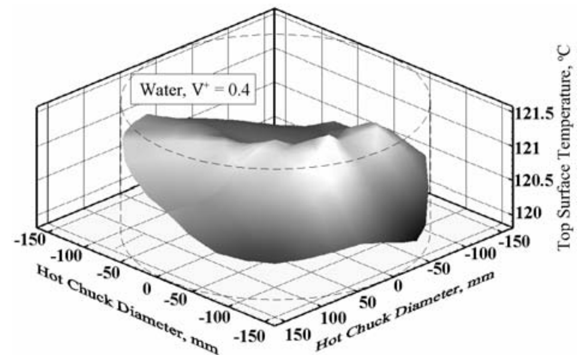

Fig. 9. Temperature profile, pure water, $V^+ = 0.4$.

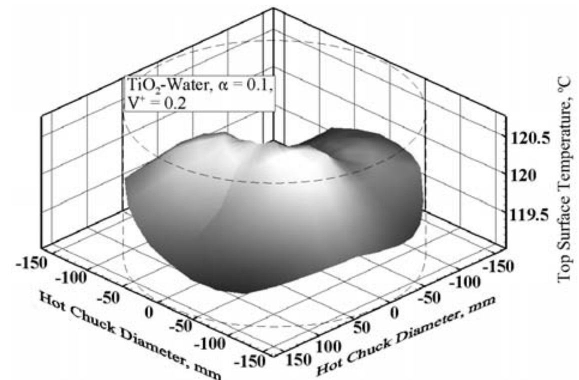

Fig. 10. Temperature Profile, TiO_2 –Water nanofluid, α =0.1, V^+=0.2.

the literature. The amount of working fluid should be enough to transfer the heat in the evaporator section as well as the amount of vapor and the returning condensate in the transporting loop and the condenser section.

In this study, the quantity of working fluid inside the HPHC was defined as the ratio of the volume of the working fluid in the heat pipe to the inside total volume. The important constraint in the operation of a thermosyphon is the effect of V^+. The quantity of the working fluid was found to vary directly with an increase or decrease of the temperature uniformity of the HPHC. There are a few analytical studies on the amount of working fluid in heat pipes, based on very simplified assumptions which grossly underestimate the real situations.

Imura et al. [14] suggested a useful formula for $V_{H,I}^+$ in terms of the average temperature of the top-inside, bottom-inside, and adiabatic wall and the critical heat flux given as:

$$q_{cr} = \frac{0.64(\rho_l/\rho_g)^{0.13}}{\left(\frac{4l_e}{d}\right)/h_{fg}\left[\sigma g \rho_g^2(\rho_l-\rho_g)\right]^{1/4}} \tag{2}$$

$$V_{H,I}^+ = \frac{V_{LP}}{V_e} = (1/5 \sim 1/3) + \frac{0.8l_{e,c}+l_a}{l_a}\left(\frac{3\mu_l l_{e,e} q_{cr}}{\rho_l^2 g h_{fg}}\right)^{1/3} + \frac{\rho_g}{\rho_l}\left[\frac{l_{e,c}+l_a}{l_{e,e}} - \frac{0.8l_{e,c}+l_a}{l_a}\left(\frac{3\mu_l l_{e,e} q_{cr}}{\rho_l^2 g h_{fg}}\right)^{1/3}\right] \tag{3}$$

$$l_{e,e} = l_{e,c} = \frac{r^2}{d} \quad (4)$$

They mentioned that 1/5-1/3 of the first term is not sufficient in the case where l_e is much less than (l_c+l_a) and concluded that a further study on the matter is needed. However, Eq. 3 is useful to estimate the minimum amount of a working fluid. Calculation can be an approximation and be made with equivalent evaporator area. To fill the correct amount of working fluid into the HPHC, the calculated amount for the current system was approximately $V_{H.I}^+ \approx 0.4$ for water. Calculation was made with equivalent l_e and l_c as 0.075 m, respectively, and with same heating surface area compared with the present HPHC and with short l_a as 0.015 m, $V_e \approx 0.45$ m^3. But the system was experimentally charged step by step from V^+ = 0. 14 to 0.5 with Imura's approximation method. The optimum amount was investigated with experimental work.

With such information, one can determine the optimum amount of a given working fluid, and a series of experiments was carried out to determine the optimum V^+. The HPHC used in the present study was designed with a very short transport zone (15 mm). The length of the condenser and evaporator is not definitely recognized. This implies that any extrapolation of the effect of V^+ for other working fluids requires caution.

Fig. 4 shows the effect of nanofluids on the temperature uniformity of the system with various amounts. However, the choice of working fluid must be considered in terms of the system vapor pressure and saturation temperature of the working fluid because the system stability depends strongly on the working fluid. The figures demonstrate that TiO_2-H_2O nanofluid (V^+ = 0.2-0.5) seems to be the best working fluid for the present application.

As shown in Figs. 5 and 6, the system operation states are observed through the temperature difference between low peak and high peak temperature, the average temperature fluctuation of the top surface. Fig. 5 shows temperature variation with different working temperature levels (70, 100, and 120°C). The HPHC shows the best temperature uniformity with TiO_2-H_2O. As shown in Figs. 5 and 6, ΔT_{p-p} is the lowest in post system with 40% charged of 0.1 % nanofluid boiling with 1.9^{o}C. Fig. 6 expresses the average temperature fluctuation on the top surface of an HPHC system. Fig. 6 shows the best stable operation state with 20 % (V^+=0.2) charged with TiO_2-H_2O (α=0.1). It shows about ±1°C of ΔT_{p-p}.

Fig. 7 shows the two-phase heat transfer performance of HPHC. The temperature difference between bottom and top surface (ΔT_{B-T}) is lowest in the case of 0.1 % (α=0.1) of TiO_2. The lower value of ΔT_{B-T} implies that the heat transfer ability to transfer heat from the heater to top surface is high. The HPHC system is two-phase system operating with a working fluid. This means that the system can be directly affected by physical characteristics of working fluids such as thermal and physical properties.

The experimental investigation of the system working stability is a direct extension of the present study. The high temperature fluctuation of an HPHC deteriorates system operation performance. The instability of the working fluid flow within the HPHC is one of the major concerns for the design of any two-phase system. Fig. 8 is showing the temperature fluctuation on the upper surface. In Fig. 8, it is seen that the temperature fluctuations with ITO as the working fluid are severe (3.12^{o}C), and lowest fluctuation (0.5^{o}C) with TiO_2. (α=0.1, V^+=0.2). With pure water, temperature fluctuation is about 1°C and the optimum amount rated in V^+ = 0.4.

Figs. 9 and 10 show a high-low temperature profile on the top surface of HPHC in a certain time. As shown in figure, the temperature in the center is higher than other positions in 300 mm circular HPHC. This must be due to the holding column in the center of the HPHC.

Fig. 11(a) shows the effect of cell structure installed in HPHC inside. It shows higher ΔT_{B-T} in case of the distilled

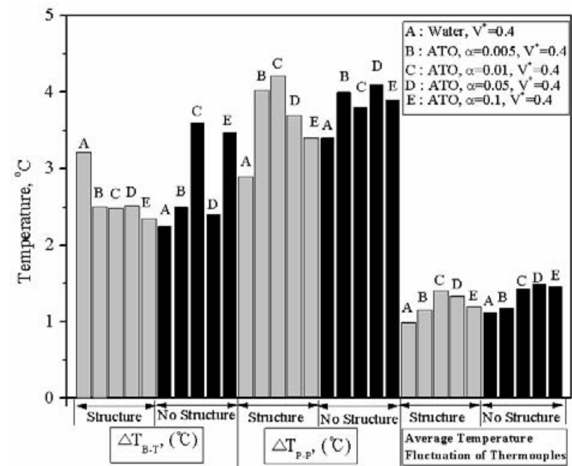

(a) Characteristic temperaturest

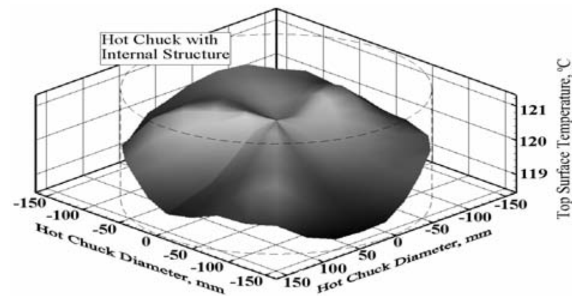

(b) With structure, water, V^+ = 0.4

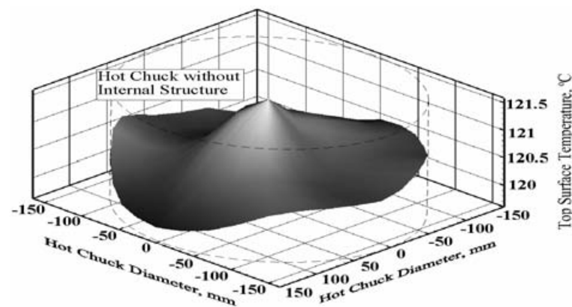

(c) Without structure, water, V^+ = 0.4

Fig. 11. Effect of internal structure of HPHC inside.

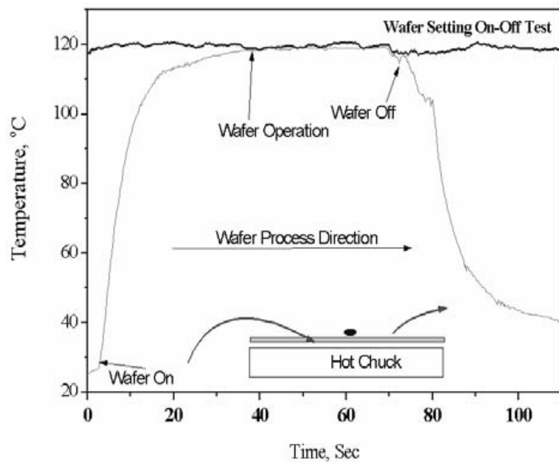

Fig. 12. Wafer operation trajectory.

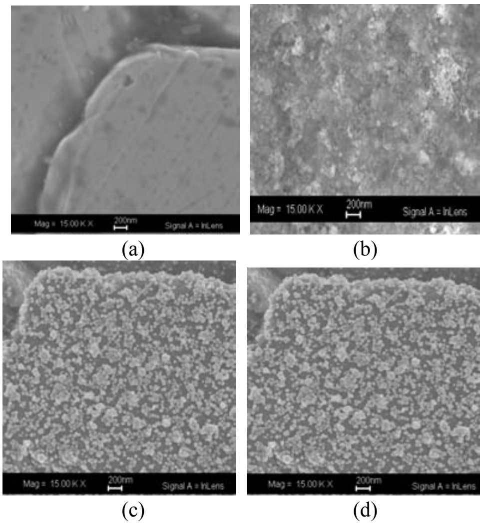

(a) Pure Surface, No nanofluid, AL701
(b) After Boiling with nanofluid (0.1%-TiO_2)
(c) After Boiling with nanofluid (0.1%-Ag)
(d) Coagulation after Al_2O_3

Fig. 13. Micro and macro view on the evaporator inside surface after nanofluids.

water than HPHC without cell structure. For ΔT_{p-p} which explains the temperature uniformity on the Upper surface, the internal structure HPHC with the distilled water and 0.1 % ATO HPHC showed better uniformity, ΔT_{p-p} with other concentration is not much different. Temperature fluctuation is slightly low compared with HPHC without internal cell structure. Also, Fig. 11(b) and (c) shows the effect of structure. As shown, HPHC without structure shows the peak temperature placed on the center. This means that the inside structures are helpful for temperature flattening on the surface and the heat from the bottom can be spread to the whole surface.

As shown in Fig. 12, even with state-of-the-art wafer operation tracks, the across-wafer temperature range can be as much as 9°C during the heating transient wafer on-off process and 0.7°C during the steady state [1]. As shown in Fig. 12, while better performance has been recorded, it is very difficult

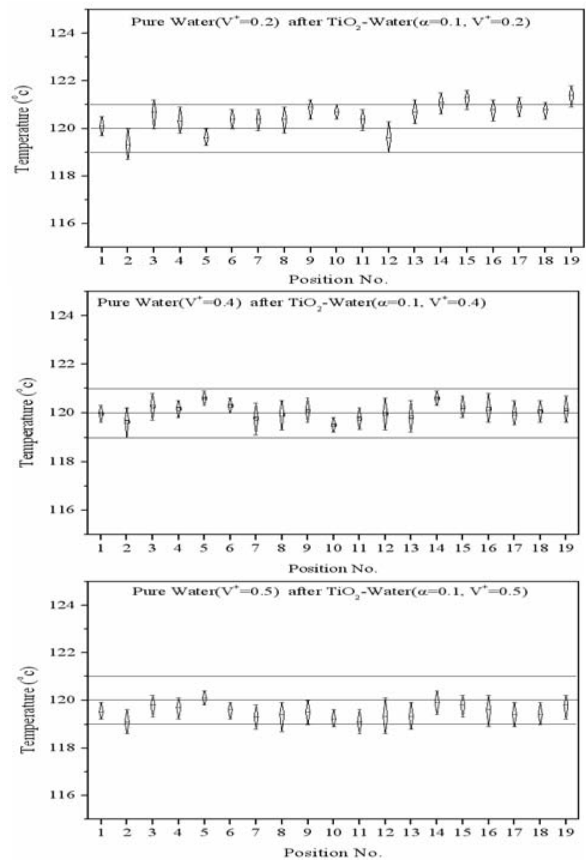

Fig. 14. Temperature profile on top surface with after boiling with various amount of nanofluid 0.1%.

to achieve good uniformity, especially during the transient phase, due to the inherent lack of temperature control during wafer transport and heating transients. More specifically, the bake step is conducted by transferring the cold wafer to the hot HPHC bake plate and the chill step follows. These transport processes between plates abruptly change the thermal behavior of the HPHC system. In the present HPHC wafer baking process, we propose a simple baking module with nanofluidic flat plate heat pipe hot chuck, which relies on a special wafer carrier to on-off transfer. This simple chuck system can help the stable wafer transfer operation without the abrupt change of surface thermal state.

Another important effect caused by nanofluid with boiling in the HPHC is the porous layer on the inside surface in evaporator side. It will increase the surface wettability. The surface wettability will increase the nucleation rate with improved contact angle on the evaporator surface. One can see the difference in the structure of the surface. As shown in Figs. 13 and 14, the difference is further illustrated by comparing the SEM images. From these images it is seen that the features created in the surface are similar with different set of tests with various amounts of working fluid [15]. A few representative cases in the present study are shown in Figs. 13 and 14. As shown in Fig. 13, the difference between (a), (b) with TiO_2 and (c) with Ag is the nanoporous layer on the surface after

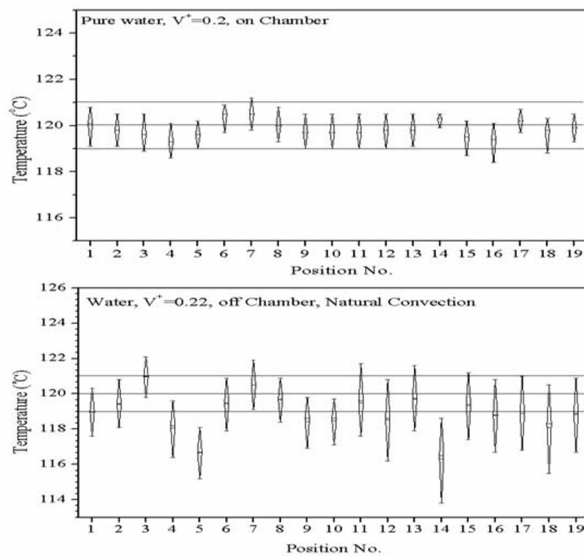

Fig. 15. Effect of temperature uniformity with chamber.

boiling of nanofluid. SEM photos after boiling nanofluid show the obvious difference. As shown in the SEM photo, the roughness and total area of the boiled surface by nanofluid are much different from those of the surface boiled in pure water. This can lead to decrease of the contact angle on the nanoporous layer and such decrease occurs with pure water as well as nanofluid droplets; thus the wettability is enhanced by the nanoporous layer on the surface, not the nanoparticles in the fluid. This phenomenon has been reported by Kim et al. [15]. Also, Fig. 13(d) shows the macro view of inside the evaporator after Al_2O_3. As shown in Fig. 13(d), a large amount of agglomeration of nanoparticles was observed. As shown in Fig. 14, the temperature profile is not much different from previous boiling results with nanofluid. This means that the surface nanoparticle deposition leads to increased nucleation rate and boiling performance.

Fig. 15 shows the effect of natural convection on the off chamber state. If HPHC is on the outside chamber, the temperature uniformity is deteriorated abruptly. This could be due to the flow non-uniformity on the top surface. This shows partially similar phenomena with Chien et al's results on flow pattern between wafer and chuck [19]. They mentioned that a uniform flow rate is needed to obtain temperature uniformity during wafer operation.

4. Conclusions

As semiconductor manufacturing technology evolves toward smaller sizes, higher temperature uniformity becomes increasingly important in the wafer baking process. This led us to develop an HPHC that exploits the superior temperature uniformity and thermal response of heat pipes for use in commercial wafer manufacturing and inspection process. The HPHC plate has a number of significant advantages:

- Exceptional temperature uniformity of ± 1°C across the effective surface area (300-mm in radius for 300-mm wafers) for a working temperature range from 70 to 120ºC was achieved.
- Excellent thermal response on the wafer on-off transfer process resulting from the smaller heat capacity of the radial empty chamber structure of heat pipe without the abrupt temperature change was achieved.
- Minimum thermal deformation of the plate because excellent thermal uniformity is maintained while the plate is being heated up to specified setting temperature.
- The optimum performance in temperature uniformity in the range of ± 1°C was achieved from nanofluidic HPHC with TiO_2 particles (α=0.1, V^+=0.5).
- It was observed that the temperature uniformity can be improved with thermosyphonic HPHC compared having cell structure.

The easy temperature uniformity of the HPHC 300 mm plate makes it especially well suited for thermal processing of semiconductor wafer baking processes that require high precision temperature control.

Acknowledgment

This research was supported by the MKE (The Ministry of Knowledge Economy), Korea, under the ITRC (Information Technology Research Center) support program supervised by the NIPA (National IT Industry Promotion Agency" (NIPA-2009- (C1090-0904-0007)).

Nomenclature

d	:	Diameter (m)
h_{fg}	:	Latent heat of vaporization (J/kg°C)
l	:	Length (m)
q	:	Heat flux (W/m^2)
r	:	Radius (m)
T	:	Temperature (°C)
TCT	:	Two-phase closed thermosyphon
ΔT_{B-T}	:	Temperature difference between bottom and top surface (°C)
ΔT_{P-P}	:	Temperature difference between low and high peak on top surface (°C)
V	:	Volume (m^3)
V_e	:	Volume of evaporator (m^3)
V_{HPHC}	:	Total effective volume (m^3)
V_{LP}	:	Volume of liquid pool (m^3)
V^+	:	Dimensionless working fluid volume, V_{LP}/V_{HPHC}
$V_{H,I}^+$	:	Dimensionless working fluid volume, V_{LP}/V_e
WF	:	Working fluid

Greek letter symbols

α	:	Nanoparticle volume concentration (%)
ϕ	:	Diameter (m)
μ	:	Viscosity (kg/m-s)
ρ	:	Density (kg/m^3)
σ	:	Surface tension (N/m)

Subscripts

a : Adiabatic section
c : Cold section
cr : Critical
e : Evaporation, evaporator
e,e : Effective evaporator
e,c : Effective condenser
g : Gas, vapor state
h : Heater, hot
l : Liquid

References

[1] Y. Hisaaki and O. Tetsuro, Development of Heat Pipe Isothermal Heating Plate, *Proceeding of 8th IHPS*, Kumamoto, Japan, (2006).

[2] Q. Zhang, P. Friedberg, K. Poolla and C. Spanos, Enhanced Spatial PEB Uniformity through a Novel Bake Plate Design, *AEC/APC XVII 2005*, (2006).

[3] Q. Zhang, P. Friedberg et al., Across Wafer CD Uniformity Enhancement through Control of Multi-zone PEB Profiles, Metrology, Inspection, and Process Control for Microlithography XVIII, *SPIE 5375*, (2004).

[4] P. Friedberg, C. Tang et al., Time-based PEB adjustment for optimizing CD distributions, Metrology, Inspection, and Process Control for Microlithography XVIII, *SPIE 5375*, (2004).

[5] D. Steele, A. Coniglio et al, Characterizing Post Exposure Bake Processing for Transient and Steady State Conditions, in the Context of Critical Dimension Control, Metrology, Inspection, and Process Control for Microlithography XVI, *SPIE 5375*, (2002).

[6] D. R. FLYNN, W. M. HEALY and R. P. ZARR, High-Temperature Guarded Hot Plate Apparatus: Optimal Locations of Circular Heaters, *International Thermal Conductivity 28th Conference/International Thermal Expansion 16th Symposium. Proceedings*, June 26-29, New Brunswick, Canada, (2005) 466-477.

[7] G. J. Park, J. O. Yang, H. S. Kwak, S. H. Park and J. J. Lee, Design and Experimental Test of a Hot Plate for Hot Embossing Nano-Imprintting Equipments, *Proceeding of KSME Annual Spring & Fall Meeting*, (2006) 2006-2011.

[8] G. J. Park, H. S. Kwak, D. W. Shin and J. J. Lee, Numerical simulation of thermal control of a hot plate for thermal nanoimprint lithography machines, *Proceeding of KSCFE Annual Fall Meeting*, (2007) 153-158.

[9] S. Y. Lee, H. H. Cho, Y. W. Lee and Lee, A study to improve Temperature Uniformity in Hot plate Oven for Silicon Wafer Manufacturing, *Journal of the KSME (B)*, 2 (2) (2000) 261-266.

[10] J. Lee and H. H. Cho, Study on Thermal Design of Hot Plate for Enhancing Temperature Uniformity, *KSME Annual Fall Meeting*, (2007) 190-194.

[11] G. J Park, J. O. Yang, H. S. Kwak and J. J. Lee, Employment of heat pipes to achieve temperature uniformity of a large-area hot-plate for TH-NIL, *KSMTE Annual Fall Meeting*, (2007) 74-79.

[12] J. H. Boo, W. B. Chung, T. G. Kim, study on the Condenser Temperature Characteristics of a Disk Type Heat Pipe, *KSME Fall Conference*, (2000) 148-153.

[13] Y. Lee, I. L. Pioro and H. J. Park, An Experimental Study on a Plate Type Two-Phase Closed Thermosyphon, *4th IHPS*, Tsukuba, Japan, (1994) 49-58.

[14] H. Imura, K. Sasaguchi and H. Kozai, Critical Heat Flux in a Two Phase Closed Thermosyphon," *Int. J. of Heat Transfer*, 26 (8) (1993) 1181-1188.

[15] S. J. Kim, I. C. Bang, J. Buongiorno and L. W. Hub, Surface wettability change during pool boiling of nanofluids and its effect on critical heat flux, *Int. J. of Heat and Mass Transfer*, 50 (19-20) (2007) 4105-4116.

[16] S. U. S. Choi, Enhancing thermal conductivity of fluids with nanoparticles, in Developments and Applications of Non-Newtonian Flows, ASME FED 231/MD 66 (1995) 99-103.

[17] S. K. Das, N. Putra and W. Roetzel, Pool boiling characterization of nano-fluids, *International Journal of Heat and Mass Transfer*, 46 (2003) 851-862.

[18] S. K. Das, N. Putra and W. Roetzel, Pool boiling nanofluids on horizontal narrow tubes, *International Journal of Multiphase Flow*, 29 (2003) 1237-1247.

[19] H. T. Chien, C. I., Tsai, P. H., Chen and P.-Y. Chen, Improvement on thermal performance of a disk shaped miniature heat pipe with nanofluid, *IEEE ICEPTD*, (2003) 381-391.

[20] C. Y. Tsai, H. T. Chien, P. P. Ding, B. Chan, T. Y. Luh and P. H. Chen, Effect of structural character of gold nanoparticles in nanofluid on heat pipe thermal performance, *Materials Letters*, 58 (2004) 1461-1465.

[21] S. W. Kang, W. C. Wei, S. H. Tsai and S. Y. Yang, Experimental investigation of silver nano-fluid on heat pipe thermal performance, *Applied Thermal Engineering*, 26 (2006) 2377-2382.

[22] H. B. Ma, S. U. S. Choi and M. Tirumala, Effect of nanofluid on the heat transport capability in an oscillating heat pipe, *Applied Physics Letters*, 88 (2006) 116-143.

Taek-Kyu Lim is a graduate student in the School of Mechanical Engineering, Chungbuk National University. He is working on heat pipe systems, CFD and heat exchangers.

Seok-Ho Rhi is an Associate Professor in Chungbuk National University and he received the Ph.D degree from the University of Ottawa, Canada. He is interested in heat pipes, heat exchangers and, thermoelectric modules.